

# Dynamics of strange, charm and high momentum hadrons in relativistic nucleus-nucleus collisions

W. Cassing<sup>1</sup>, K. Gallmeister<sup>1</sup>, E. L. Bratkovskaya<sup>\*2</sup>, C. Greiner<sup>2</sup>, and H. Stöcker<sup>2</sup>

<sup>1</sup>Institut für Theoretische Physik, Universität Giessen, Germany

<sup>2</sup>Institut für Theoretische Physik, Universität Frankfurt, Germany

## Abstract

We investigate hadron production and attenuation of hadrons with strange and charm quarks (or antiquarks) as well as high transverse momentum hadrons in relativistic nucleus-nucleus collisions from  $2 \text{ A}\cdot\text{GeV}$  to  $21.3 \text{ A}\cdot\text{TeV}$  within two independent transport approaches (UrQMD and HSD). Both transport models are based on quark, diquark, string and hadronic degrees of freedom, but do not include any explicit phase transition to a quark-gluon plasma. From our dynamical calculations we find that both models do not describe the maximum in the  $K^+/\pi^+$  ratio at 20 - 30  $\text{A}\cdot\text{GeV}$  in central Au+Au collisions found experimentally, though the excitation functions of strange mesons are reproduced well in HSD and UrQMD. Furthermore, the transport calculations show that the charmonium recreation by  $D + \bar{D} \rightarrow J/\Psi + \text{meson}$  reactions is comparable to the dissociation by 'comoving' mesons at RHIC energies contrary to SPS energies. This leads to the final result that the total  $J/\Psi$  suppression as a function of centrality at RHIC should be less than the suppression seen at SPS energies where the 'comover' dissociation is substantial and the backward channels play no role. Furthermore, our transport calculations – in comparison to experimental data on transverse momentum spectra from  $pp$ , d+Au and Au+Au reactions – show that pre-hadronic effects are responsible for both the hardening of the hadron spectra for low transverse momenta (Cronin effect) as well as the suppression of high  $p_T$  hadrons. The mutual interactions of formed hadrons are found to be negligible in central Au+Au collisions at  $\sqrt{s} = 200 \text{ GeV}$  for  $p_T \geq 6 \text{ GeV}/c$  and the sizeable suppression seen experimentally is attributed to a large extent to the interactions of 'leading' pre-hadrons with the dense environment.

## 1 Introduction

The dynamics of ultra-relativistic nucleus-nucleus collisions at AGS, SPS and RHIC energies are of fundamental interest with respect to the properties of hadronic/partonic systems at high energy densities as encountered in the early phase of the 'big bang'. Especially the formation of a quark-gluon plasma (QGP) and its transition to interacting hadronic matter has motivated a large community for about 20 to 30 years by now [1]. However, even after more than a decade of experiments at the SPS and in the last years at RHIC the complexity of the dynamics has not been unraveled and no conclusive evidence has been obtained for the formation of the QGP and/or the properties of the phase transition.

---

<sup>\*</sup>Supported by DFG

Apart from the light and strange flavor ( $u, \bar{u}, d, \bar{d}, s, \bar{s}$ ) quark physics and their hadronic bound states in the vacuum ( $\pi, K, \phi$  etc.) the interest in hadronic states with charm flavors ( $c, \bar{c}$ ) has been rising additionally in line with the development of new experimental facilities. This relates to the charm production cross section in  $pN$ ,  $\pi N$ ,  $pA$  and  $AA$  reactions as well as to their interactions with baryons and mesons which determine their properties (spectral functions) in the hadronic medium. Especially the  $J/\Psi$  suppression at SPS energies has been discussed as a signature for a QGP phase due to Debye screening [2]. On the other hand, it has been pointed out - within statistical models - that at RHIC energies the charmonium formation from open charm + anticharm mesons might become essential [3, 4] and even exceed the yield from primary  $NN$  collisions. Thus charmonium suppression or enhancement is of central importance for an understanding of nucleus-nucleus collisions at RHIC energies.

Additionally, transverse mass (or momentum) spectra of hadrons are in the center of interest. On the one hand the suppression of high transverse momentum hadrons is investigated in  $Au+Au$  reactions relative to  $pp$  collisions at RHIC energies of  $\sqrt{s} = 200$  GeV [5], since the propagation of a fast quark through a hot colored medium (QGP) should be different than in ordinary high density hadron matter [6, 7]. In fact, the PHENIX [8] and STAR [9] collaborations have reported a large relative suppression of hadron spectra for transverse momenta  $p_T$  above  $\sim 3\text{-}4$  GeV/c which might point towards the creation of a QGP, since this suppression is not observed in  $d+Au$  interactions at the same bombarding energy per nucleon [10, 11]. But it is not clear presently, to which extent this suppression might be due to ordinary hadronic final state interactions [12], too. On the other hand, the measured transverse mass ( $m_T -$ ) spectra of kaons at AGS and SPS energies show the opposite behavior for *soft* hadrons, i.e. a substantial *hardening* of the spectra in central  $Au+Au$  collisions relative to  $pp$  interactions (cf. also [13]). The *flat* spectra observed are commonly attributed to strong collective flow that is absent in the respective  $pp$  or  $pA$  data. An open question currently is, if the collective flow seen experimentally might be attributed to final state interactions of formed hadrons, too.

In our studies we use two independent transport models that employ hadronic and string degrees of freedom, i.e. UrQMD [14, 15] and HSD [16, 17]. They take into account the formation and multiple rescattering of hadrons and thus dynamically describe the generation of pressure in the early phase - dominated by strings - and the hadronic expansion phase. Both transport approaches are matched to reproduce the nucleon-nucleon, meson-nucleon and meson-meson cross section data in a wide kinematic range. We point out explicitly, that no parton-parton scattering processes are included in the studies below contrary to the multi-phase transport model (AMPT) [18], which is currently employed from upper SPS to RHIC energies. Whereas the underlying concepts of UrQMD and HSD are very similar, the actual realizations differ considerably.

## 2 Strange and charm hadrons

### 2.1 Numerical implementation of 'hard' probes

Whereas the dynamics of hadrons with  $u, d, s$  (and  $\bar{u}, \bar{d}, \bar{s}$ ) quarks is described nonperturbatively in HSD and UrQMD, the dynamics of 'rare' species needs a perturbative modeling in order to achieve acceptable statistics. For the production and propagation of open charm mesons, charmonia or hadrons with high transverse momentum ( $> 2.0$  GeV/c) we employ the perturbative scheme as used in Refs. [19, 20, 21, 22]. We recall that initial hard processes (such as  $c\bar{c}$ , Drell-Yan or high  $p_T$  hadron production from  $NN$  collisions) are 'precalculated' to achieve a scaling of the inclusive cross section with the number of projectile and target nucleons as  $A_P \times A_T$  when integrating over impact parameter (cf. Ref. [20]). Each open charm meson, charmonium or high  $p_T$  hadron is produced in the transport calculation with a weight  $W_i$  given by the ratio of the actual production cross section divided by the inelastic nucleon-

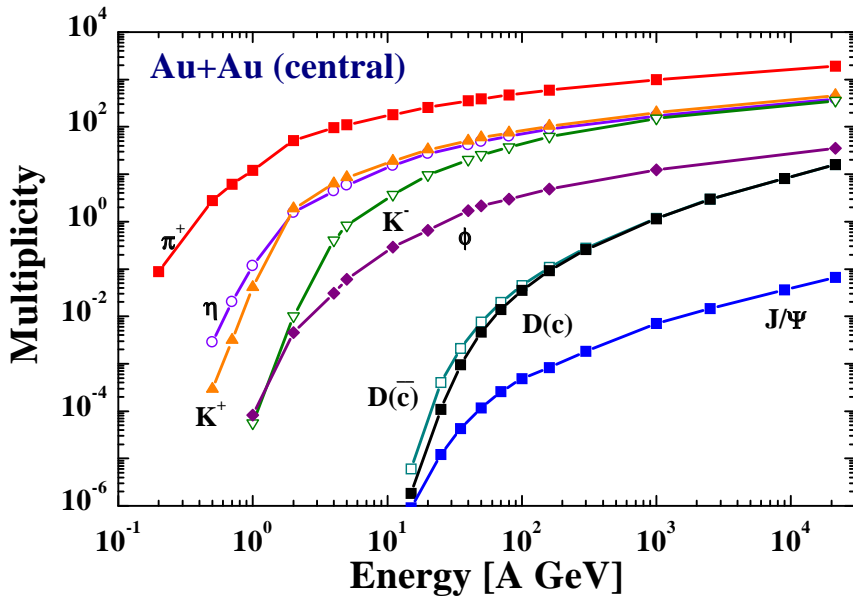


Figure 1: The multiplicities for  $\pi^+$ ,  $\eta$ ,  $K^+$ ,  $K^-$ ,  $\phi$ ,  $D$ ,  $\bar{D}$  and  $J/\Psi$ -mesons for central collisions of  $Au + Au$  as a function of bombarding energy. In the HSD calculations elastic and inelastic reactions of all hadrons are included, but no in-medium modifications of their spectral functions (The figure is taken from Ref. [20]).

nucleon cross section, i.e.

$$W_i = \frac{\sigma_{NN \rightarrow h(p_T) + x}(\sqrt{s})}{\sigma_{NN}^{inelas.}(\sqrt{s})}. \quad (1)$$

We then follow the motion of these hadrons within the full background of strings/hadrons by propagating them as free particles, i.e. neglecting in-medium potentials, but compute their collisional history with baryons and mesons or quarks and diquarks. For reactions with diquarks we use the corresponding reaction cross section with baryons multiplied by a factor of 2/3. For collisions with quarks (antiquarks) we adopt half of the cross section for collisions with mesons and for the leading quark (formed) baryon collision a factor of 1/3 is assumed. The final states in an inelastic collision are then modeled by the JETSET fragmentation scheme in the same way as for ordinary hadron-hadron collisions.

## 2.2 Excitation functions of mesons in central collisions of heavy nuclei

In order to provide an overview on meson production we show in Fig. 1 the calculated excitation function of  $\pi^+$ ,  $K^\pm$ ,  $\eta$ ,  $\phi$ ,  $D$ ,  $\bar{D}$  and  $J/\Psi$  mesons in central  $Au + Au$  collisions from lower SIS to top RHIC energies without employing any self energies for these mesons in the HSD transport approach (cf. Ref. [19, 20]). We mention that the excitation functions of the strange hadrons from HSD and UrQMD match rather well with the data available, however, the sharp maximum in the  $K^+/\pi^+$  ratio at  $\sim 20$  to  $30$  A·GeV in central  $Au+Au$  (Pb+Pb) collisions is missed [23]. This also holds for the slope of the  $K^\pm$  transverse mass spectra above  $\sim 5$  A·GeV in central  $Au+Au$  (Pb+Pb) collisions [24, 25].

The  $\bar{D}$ -mesons with a  $\bar{c}$  are produced more frequently at low energies due to the associated production with  $\Lambda_c$ ,  $\Sigma_c$ ,  $\Sigma_c^*$  similar to the kaon case, where kaon+hyperon production is more frequent than  $K + \bar{K}$  production. At roughly 15 A·GeV the cross sections for open charm and charmonia are similar, while the ratio of open charm to charmonium bound states increases rapidly with energy. Again, this behaviour is comparable to the excitation functions in the strangeness sector when comparing  $K^+$ ,  $K^-$  and  $\phi$ -mesons. Since the excitation function for open charm drops very fast with decreasing bombarding energy, experiments at 20 to 30 A·GeV at the future GSI facility will be a challenging task since the multiplicity of the other mesons is higher by orders of magnitude. On the other hand, the perspectives for open charm measurements at RHIC appear promising since about 15  $c\bar{c}$  (or  $D\bar{D}$ ) pairs should be created in central  $Au + Au$  collisions at  $\sqrt{s} = 200$  GeV according to the HSD transport calculations.

## 2.3 Open charm and charmonia at SPS and RHIC

We calculate open charm and charmonium production at SPS and RHIC energies (within the HSD transport approach for the overall reaction dynamics) using parametrizations for the elementary production channels including the charmed hadrons  $D, \bar{D}, D^*, \bar{D}^*, D_s, \bar{D}_s, D_s^*, \bar{D}_s^*$ ,  $J/\Psi, \Psi(2S), \chi_{2c}$  from  $NN$  and  $\pi N$  collisions. The latter parametrizations are fitted to PYTHIA calculations [26] above  $\sqrt{s} = 10$  GeV and extrapolated to the individual thresholds, while the absolute strength of the cross sections is fixed by the experimental data as described in Ref. [20]. We here report on an extension of previous works [19, 22, 27] and include explicitly the backward channels 'charm + anticharm meson  $\rightarrow$  charmonia + meson' employing detailed balance in a more schematic interaction model with a single parameter or matrix element  $|M|^2$ , that is fixed by the  $J/\Psi$  suppression data from the NA50 collaboration at SPS energies (cf. Ref. [28]).

Since the meson-meson dissociation and backward reactions typically occur with low relative momenta ('comovers') it is legitimate to write the cross section for the process  $m_1 + m_2 \rightarrow m_3 + m_4$  as

$$\sigma_{1+2 \rightarrow 3+4}(\sqrt{s}) = \frac{E_1 E_2 E_3 E_4}{s} |M_f|^2 \left( \frac{M_3 + M_4}{\sqrt{s}} \right)^6 \frac{P_f}{P_i}, \quad (2)$$

where  $E_i$  and  $S_i$  denote the energy and spin of hadron  $i$ , respectively, while  $P_i$  and  $P_f$  are the initial and final momenta for fixed invariant energy  $\sqrt{s}$ . In (2)  $|M_f|^2$  stands for the effective matrix element squared, which for the different 2-body channels is taken of the form

$$\begin{aligned} |M_f|^2 &= M_0^2 && \text{for } (\pi, \rho) + J/\Psi \rightarrow D + \bar{D} \\ |M_f|^2 &= 3M_0^2 && \text{for } (\pi, \rho) + J/\Psi \rightarrow D^* + \bar{D}, D + \bar{D}^*, D^* + \bar{D}^* \\ |M_f|^2 &= \frac{1}{3}M_0^2 && \text{for } (K, K^*) + J/\Psi \rightarrow D_s + \bar{D}, \bar{D}_s + D \\ |M_f|^2 &= M_0^2 && \text{for } (K, K^*) + J/\Psi \rightarrow D_s + \bar{D}^*, \bar{D}_s + D^*, D_s^* + \bar{D}, \bar{D}_s^* + D, \bar{D}_s^* + D^* \end{aligned} \quad (3)$$

involving a single parameter  $M_0^2$  (cf. [28] and Refs. therein). The relative factors of 3 in (3) are guided by the sum rule studies in [29] which suggest that the cross section is increased whenever a vector meson  $D^*$  or  $\bar{D}^*$  appears in the final channel while another factor of 1/3 is introduced for each  $s$  or  $\bar{s}$  quark involved. The factor  $((M_3 + M_4)/\sqrt{s})^6$  in (2) accounts for the suppression of binary channels with increasing  $\sqrt{s}$  and has been fitted to the experimental data for the reactions  $\pi + N \rightarrow \rho + N, \omega + N, \Phi + N, K^+ + \Lambda$  in Ref. [30]. The advantage of the model introduced in (2) is that detailed balance for the binary reactions can be employed strictly for each individual channel and the role of the backward reactions ( $J/\Psi$ +meson formation by  $D + \bar{D}$  flavor exchange) can be explored without introducing any additional parameter once  $M_0^2$  is fixed.

We directly step on with the results for the charmonium suppression and start with the system  $Pb + Pb$  at 160 A GeV to demonstrate that the 'late' comover dissociation model (2) is approximately in line with the data of the NA50 Collaboration. The corresponding  $J/\Psi$  suppression (in terms of the  $\mu^+ \mu^-$  decay branch relative to the Drell-Yan background from 2.9 – 4.5 GeV invariant mass) as a function of the transverse energy  $E_T$  in  $Pb + Pb$  collisions at 160 A GeV is shown in Fig. 2. The solid line stands for the HSD result within the comover absorption scenario for the cross sections defined by (2) while the various data points reflect the preliminary NA50 data from the year 2000 (analysis A,B,C). A comparable agreement with the data is also achieved within the UrQMD model [27] (dashed histogram in Fig. 2). We mention that there might be alternative explanations for  $J/\Psi$  suppression as discussed in Refs. [31, 32] and/or further dissociation mechanism not considered here. However, for the purposes of the present study it is sufficient to point out that the cross sections employed here (cf. Figs. 6 and 7 in [28]) most likely are upper limits and do not lead to a sizeable recreation of charmonia by  $D + \bar{D}$  channels at SPS energies.

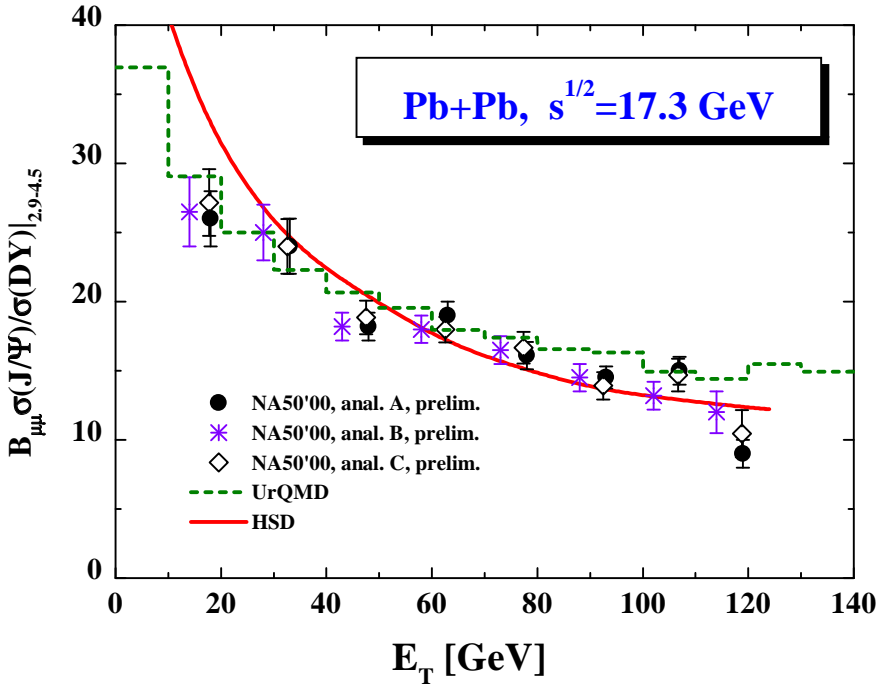


Figure 2: The  $J/\Psi$  suppression (in terms of the  $\mu^+\mu^-$  decay branch relative to the Drell-Yan background from 2.9 – 4.5 GeV invariant mass) as a function of the transverse energy  $E_T$  in  $Pb + Pb$  collisions at 160 A GeV. The solid line shows the HSD result within the comover absorption scenario presented in Section 2.3 [28]. The different symbols stand for the NA50 data [33] from the year 2000 (analysis A,B,C) while the dashed histogram is the UrQMD result from Ref. [27].

For central  $Au + Au$  collisions at  $\sqrt{s} = 200$  GeV, however, the multiplicity of open charm pairs should be about 2 orders of magnitude larger than at 160 A·GeV (according to Fig. 1), such that a much higher  $J/\Psi$  reformation rate ( $\sim N_{cc}^2$ ) is expected at RHIC energies (cf. Ref. [32]). In Fig. 3 we display the total  $J/\Psi$  comover absorption rate (solid histogram) in comparison to the  $J/\Psi$  reformation rate (dashed histogram) as a function of time in the center-of-mass frame for central  $Au+Au$  collisions at  $\sqrt{s} = 200$  GeV. The two rates become comparable for  $t \geq 4.5$  fm/c and suggest that at the full RHIC energy of  $\sqrt{s} = 200$  GeV the  $J/\Psi$  comover dissociation is no longer important since the charmonia dissociated in this channel are approximately recreated in the backward channels. Accordingly, the  $J/\Psi$  dissociation at RHIC should be less pronounced than at SPS energies. Moreover, there is even a small excess of  $J/\Psi$  formation by  $D + \bar{D}$  reactions in the first 2 fm/c.

The preliminary data of the PHENIX Collaboration [34] allow for a first glance at the situation encountered in  $Au + Au$  collisions at  $\sqrt{s} = 200$  GeV. In order to compare with the preliminary data we have performed a rapidity cut  $\Delta y \leq 2$  in the calculations. In Fig. 4 the  $J/\Psi$  multiplicity per binary collision (times the branching ratio  $B$ ) is shown as a function of the number of participating nucleons in comparison to the data at midrapidity. Since the statistics is quite limited so far on the experimental side, no final conclusion can presently be drawn, however, the data neither suggest a dramatic enhancement of  $J/\Psi$  production nor a complete 'melting' of the charmonia in the QGP phase.

### 3 High $p_T$ hadron suppression

Before coming to actual calculations for deuteron-nucleus or nucleus-nucleus collisions it is important to briefly explain the concept of 'leading' and 'secondary' hadrons in the transport approaches, since this separation is of central importance for the results to be discussed below. To this aim we recall that in a high energy nucleon-nucleon collision two (or more) color-neutral strings are assumed to be formed, which phenomenologically describe the low energy 'coherent' gluon dynamics by means of a color electric field, which is stretched between the colored ends of each single string. The latter string ends are defined by the space-time coordinates of the constituents, i.e. a diquark and quark for a

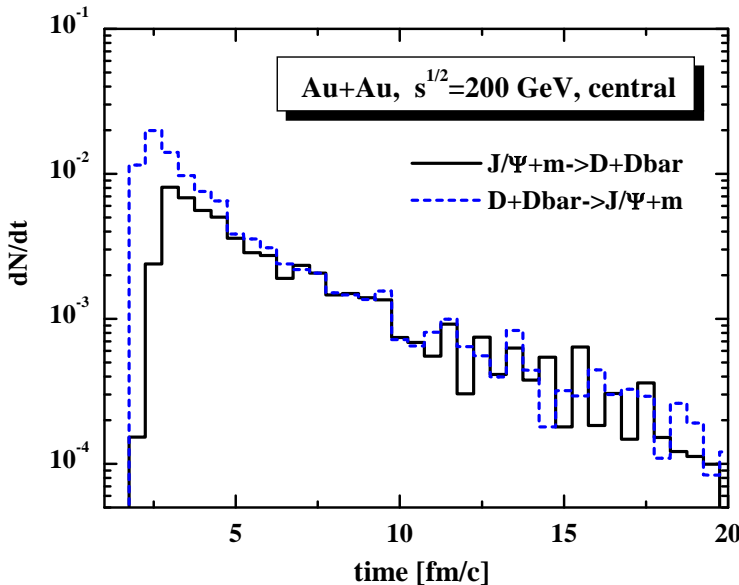


Figure 3: The calculated rate of  $J/\Psi$  dissociation reactions with mesons (solid histogram) for central  $Au + Au$  collisions at  $\sqrt{s} = 200$  GeV in comparison to the rate of backward reactions of open charm pairs to  $J/\Psi +$  meson (dashed histogram) according to the model specified in Section 2.3 (taken from Ref. [28]).

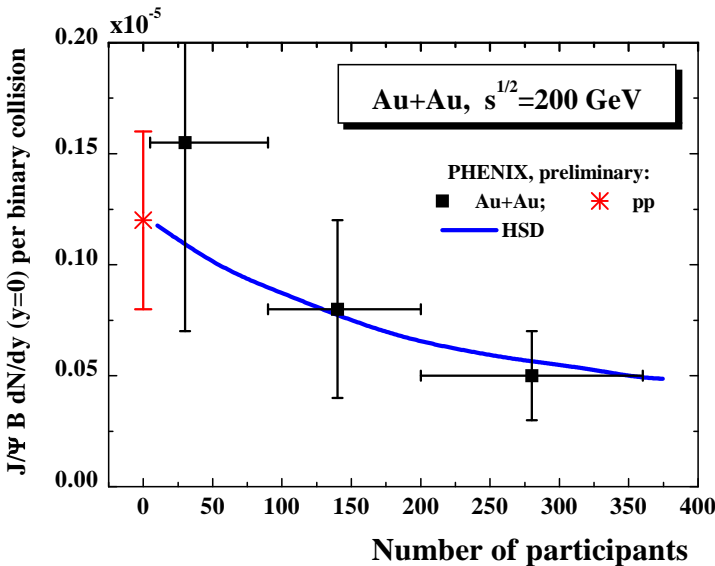


Figure 4: The calculated  $J/\Psi$  multiplicity per binary collision – multiplied by the branching to dileptons – as a function of the number of participating nucleons  $N_{part}$  in comparison to the preliminary data from the PHENIX Collaboration [34] for  $Au + Au$  and  $pp$  reactions (taken from Ref. [28]).

'baryonic' string or quark and antiquark for a 'mesonic' string. These constituents quarks (diquarks or antiquarks) are denoted as 'leading' quarks that constitute the 'leading' pre-hadrons.

The time that is needed for the fragmentation of the strings and for the hadronization of the fragments we denote as *formation time*  $\tau_f$ . For simplicity we assume (in HSD), that the formation time is a constant  $\tau_f$  in the rest frame of each hadron and that it does not depend on the particle species. We recall, that due to time dilatation the formation time  $t_f$  in any reference frame is then proportional to the Lorentz  $\gamma$ -factor, i.e.  $t_f = \gamma \cdot \tau_f$ . The size of  $\tau_f$  can be estimated by the time that the constituents of the hadrons (with velocity  $c$ ) need to travel a distance of a typical hadronic radius (0.5–0.8 fm).

We assume that hadrons, whose constituent quarks and antiquarks are created from the vacuum in the string fragmentation, do *not interact* with the surrounding nuclear medium within their formation time  $t_f$ . For the leading pre-hadrons, i.e. those involving quarks (antiquarks) from the struck nucleons, we adopt a reduced effective cross section  $\sigma_{lead}$  during the formation time  $t_f$  and the full hadronic cross section later on. Due to time dilatation light particles emerging from the middle of the string might escape the hadronic fireball without further interaction if they carry a high momentum relative to the rest frame of the fireball. However, the hadrons with transverse momenta larger than  $\sim 6$  GeV/c

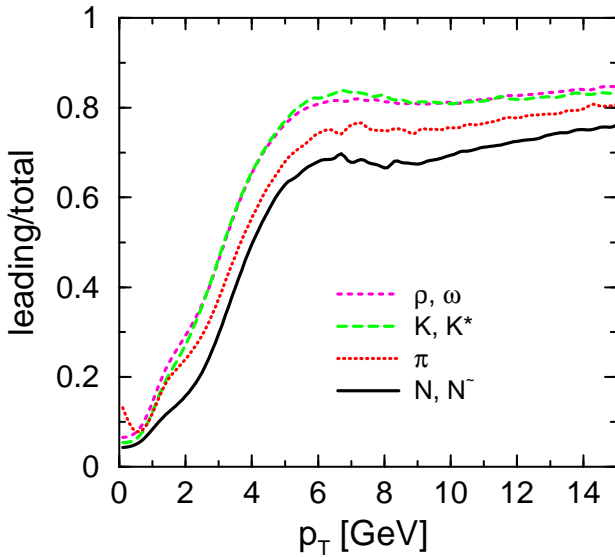


Figure 5: The ratio of 'leading particles' to 'all produced particles' in  $N + N$  collisions ( $\sqrt{s}=200$  GeV) at midrapidity for different particle classes as a function of transverse momentum within the PYTHIA model (taken from Ref. [35]).

predominantly stem from the string ends [35] and therefore can interact directly with a reduced cross section (see below).

The relative quark counting factors of 2/3 or 1/3 for the interactions of a 'leading' pre-hadron with a baryon or meson mentioned above might appear arbitrary and simplistic. However, this concept has been proven to work rather well for nucleus-nucleus collisions from SPS to RHIC energies [23, 28] as well as in hadron formation and attenuation in deep inelastic lepton scattering off nuclei [36]. Especially the latter reactions are important to understand the attenuation of hadrons with high (longitudinal) momentum in ordinary cold nuclear matter. The studies in Ref. [36] have demonstrated that the dominant final state interactions (FSI) of the hadrons with maximum momentum - as measured by the HERMES Collaboration [37] - are compatible with the concepts described above. This also holds for antiproton production and attenuation in proton-nucleus collisions at AGS energies [38]. Both independent studies point towards a hadron formation time  $\tau_f$  in the order of 0.4 to 0.8 fm/c.

As mentioned above, the question of relevance is the fraction of leading pre-hadrons as a function of transverse momentum  $p_T$  for the different hadron species. This information is extracted from PYTHIA calculations and displayed in Fig. 5 for  $pp$  collisions at  $\sqrt{s} = 200$  GeV. Here one notices slight differences between pions and especially antibaryons, however, the fraction of leading pre-hadrons increases with  $p_T$  and saturates above  $\sim 6$  GeV/c. Thus at high momenta the major fraction of 'hadrons' is of leading quark, antiquark or diquark origin and - according to the assumptions stated above - may interact without delay with the partonic/hadronic environment.

### 3.1 $d + Au$ collisions at RHIC

As pointed out before (cf. Ref. [24]) the slope of the transverse mass spectra especially of kaons and antikaons at SPS and RHIC energies is severely underestimated by the conventional transport approaches HSD and UrQMD when including only hadronic reinteractions of secondary mesons. However, as known from the experimental studies of Refs. [39, 40] an enhancement of the transverse momentum cross section from  $p + A$  collisions relative to scaled  $pp$  collisions is already observed at ISR energies. This 'Cronin effect' is presently not fully understood in its details, but most likely related to an increase of the average transverse momentum squared  $\langle k_T^2 \rangle$  of the partons in the nuclear medium prior to the 'hard' scattering vertex. We speculate that such an enhancement of  $\langle k_T^2 \rangle$  might be related to initial semi-hard gluon radiation of the leading parton in the medium, which is reduced in the vacuum due to color neutrality in a small volume. Since the microscopic mechanisms are beyond the scope of our

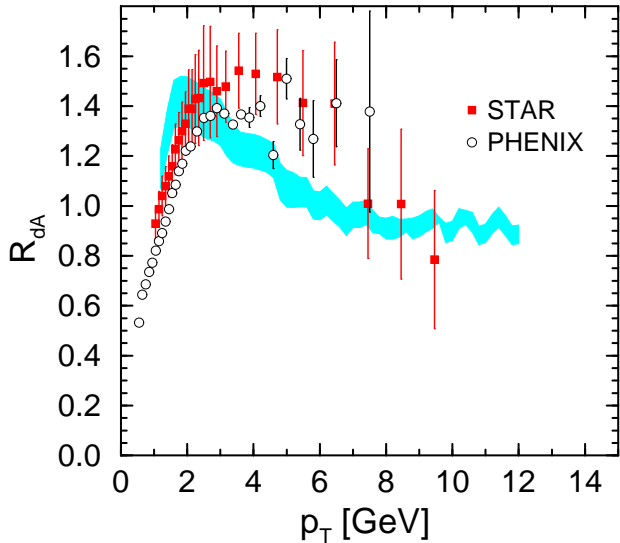


Figure 6: The suppression factor  $R_{dA}$  (5) for minimum bias  $d + Au$  collisions ( $\sqrt{s}=200$  GeV) at midrapidity. Experimental data are from PHENIX [10] (open circles) and STAR [11] (filled squares), while the hatched band shows the calculated charged hadron ratio (taken from Ref. [35]).

present analysis, we simulate this effect in the transport approach by increasing the average  $\langle k_T^2 \rangle$  in the string fragmentation function with the number of previous collisions  $N_{prev}$  as

$$\langle k_T^2 \rangle = \langle k_T^2 \rangle_{pp} (1 + \alpha N_{prev}). \quad (4)$$

The parameter  $\alpha \approx 0.25 - 0.4$  is fixed in comparison to the experimental data for  $d + Au$  collisions [10, 11] (cf. Fig. 6).

A comparison of the calculated ratio

$$R_{dA}(p_T) = \frac{1/N_{dA}^{event} d^2 N_{dA}/dydp_T}{\langle N_{coll} \rangle / \sigma_{pp}^{inelas} d^2 \sigma_{pp}/dydp_T} \quad (5)$$

is shown in Fig. 6 with the respective data for charged hadrons from Refs. [10, 11] for  $\alpha = 0.25 - 0.4$  (hatched band). In (5)  $\langle N_{coll} \rangle \approx 8.5$  denotes the number of inelastic nucleon-nucleon collisions per event (for minimum bias collisions), whereas  $\sigma_{pp}^{inelas}$  denotes the inelastic  $pp$  cross section ( $\approx 42$  mb). We find that the HSD calculations give a rise in the ratio (5) for small  $p_T$  and a decrease for  $p_T \geq 2.5$  GeV/c. The hatched band gives an estimate for the systematic uncertainty in (4) with respect to the strength of the Cronin effect that carries over to studies for  $Au + Au$  reactions (see below). The important issue in this context is that no dramatic absorption of high  $p_T$  hadrons is found in the calculations as well as in the data.

### 3.2 $Au + Au$ collisions at RHIC

We step on with 5% central  $Au + Au$  collisions at  $\sqrt{s} = 200$  GeV. For  $Au + Au$  collisions we define the nuclear modification factor in accordance with eq. (5) as

$$R_{AA}(p_T) = \frac{1/N_{AA}^{event} d^2 N_{AA}/dydp_T}{\langle N_{coll} \rangle / \sigma_{pp}^{inelas} d^2 \sigma_{pp}/dydp_T}. \quad (6)$$

Fig. 7 shows a comparison of the calculations for eq. (6) with the data for charged hadrons from Refs. [8, 9]. The surprising result in Fig. 7 is that the ratio  $R_{AA}$  is roughly described in shape for the default HSD parameters (formation time  $\tau_F = 0.8$  fm/c) within the uncertainties of the 'Cronin' simulations. Only the absolute magnitude of the high  $p_T$  suppression seen experimentally is slightly underestimated. In order to understand this result we have decomposed the ratio  $R_{AA}$  into contributions from secondary

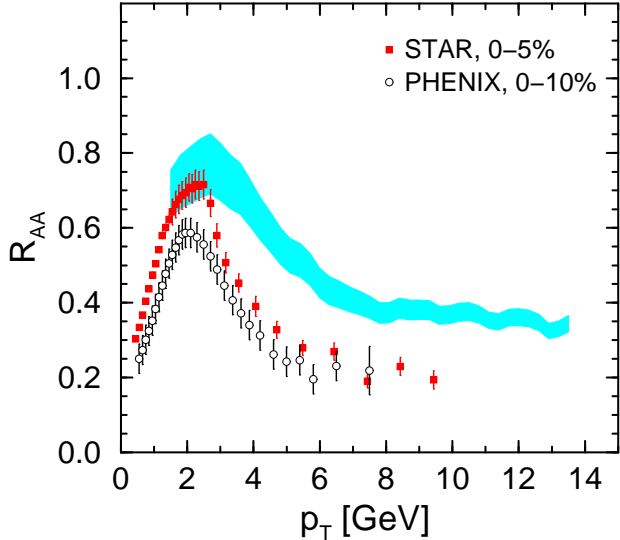


Figure 7: The suppression factor  $R_{AA}$  (6) of charged hadrons at 5% (or 10%) central  $Au + Au$  collisions ( $\sqrt{s}=200$  GeV) at midrapidity for  $\alpha = 0.25$  to 0.4 (hatched band). The experimental data are from Refs. [8, 9] and show some additional suppression mechanism, which might be attributed to partonic interactions in a colored medium (taken from Ref. [35]).

pions, kaons and  $\rho, \omega, K^*$  vector mesons (before decays) as well as from leading pre-hadrons. We find that formation time effects play a substantial role since heavier hadrons are formed earlier than light pions in the cms frame at fixed transverse momentum due to the lower Lorentz boost. However, the total suppression by scatterings of formed hadrons is negligible for  $p_T \geq 6$  GeV/c and only of relevance at lower  $p_T$  for the shape of  $R_{AA}(p_T)$ . Furthermore, the attenuation of the leading pre-hadrons is roughly independent on  $p_T$  and hadron type and gives  $R_{AA} \approx 0.1$ . Thus a large part of the attenuation seen experimentally should be addressed to the interactions of leading pre-hadrons with already formed hadrons. Nevertheless, the experimental data indicate some additional suppression mechanism.

## 4 Conclusions

Summarizing this contribution, we point out that strange hadron production in central  $Au+Au$  (or  $Pb+Pb$ ) collisions is quite well described in the independent transport approaches HSD and UrQMD [23]. The exception are the pion rapidity spectra at the highest AGS energy and lower SPS energies, which are overestimated by both models. As a consequence the HSD and UrQMD transport approaches underestimate the experimental maximum of the  $K^+/\pi^+$  ratio at  $\sim 20$ - $30$  A·GeV [23, 25].

Furthermore, the transport calculations show that the charmonium recreation by  $D + \bar{D} \rightarrow J/\Psi + \text{meson}$  reactions is comparable to the dissociation by 'comoving' mesons at RHIC energies contrary to SPS energies. This leads to the final result that the total  $J/\Psi$  suppression as a function of centrality at RHIC should be less than the suppression seen at SPS energies where the 'comover' dissociation is substantial and the backward channels play no role. Since the statistics is quite limited in the present experiments for the  $J/\Psi$  yield versus centrality, no final conclusion can be drawn so far; however, the available data neither suggest a dramatic enhancement of  $J/\Psi$  production nor a complete 'melting' of the charmonia in a QGP phase [28].

Moreover, our transport calculations in comparison to experimental data on high transverse momentum spectra from  $d+Au$  and  $Au+Au$  reactions show that pre-hadronic effects are responsible for both the hardening of the spectra for low transverse momenta [41] (Cronin effect) as well as the suppression of high  $p_T$  hadrons [35]. The interactions of formed hadrons are found to be negligible in central  $Au+Au$  collisions at  $\sqrt{s} = 200$  GeV for  $p_T \geq 6$  GeV/c and the large suppression seen experimentally is attributed to a large extent to the interactions of 'leading' pre-hadrons with the dense environment, which should be partly of partonic nature in order to explain the large attenuation seen in central  $Au+Au$  collisions.

## References

- [1] *Quark Matter 2002*, *Nucl. Phys. A* **715** (2003) 1.
- [2] T. Matsui and H. Satz, *Phys. Lett. B* **178** (1986) 416.
- [3] R. L. Thews, M. Schroedter, and J. Rafelski, *Phys. Rev. C* **63** (2001) 054905.
- [4] M. I. Gorenstein *et al.*, *J. Phys. G* **28** (2002) 2151.
- [5] J. L. Nagle and T. S. Ullrich, preprint nucl-ex/0203007.
- [6] X. N. Wang, *Phys. Rev. C* **58** (1998) 2321.
- [7] R. Baier *et al.*, *Ann. Rev. Nucl. Part. Sci.* **50** (2000) 37.
- [8] S. S. Adler *et al.*, PHENIX Collaboration, preprint nucl-ex/0308006.
- [9] J. Adams *et al.*, STAR Collaboration, *Phys. Rev. Lett.* **91** (2003) 172302.
- [10] S. S. Adler *et al.*, PHENIX Collaboration, *Phys. Rev. Lett.* **91** (2003) 072303.
- [11] J. Adams *et al.*, STAR Collaboration, *Phys. Rev. Lett.* **91** (2003) 072304.
- [12] K. Gallmeister, C. Greiner, and Z. Xu, *Phys. Rev. C* **67** (2003) 044905.
- [13] M. I. Gorenstein, M. Gazdzicki, and K. Bugaev, *Phys. Lett. B* **567** (2003) 175.
- [14] S.A. Bass *et al.*, *Prog. Part. Nucl. Phys.* **42** (1998) 279.
- [15] M. Bleicher *et al.*, *J. Phys. G* **25** (1999) 1859.
- [16] J. Geiss *et al.*, *Nucl. Phys. A* **644** (1998) 107.
- [17] W. Cassing and E. L. Bratkovskaya, *Phys. Rep.* **308** (1999) 65.
- [18] Z. W. Lin *et al.*, *Nucl. Phys. A* **698** (2002) 375.
- [19] W. Cassing, E. L. Bratkovskaya, and S. Juchem, *Nucl. Phys. A* **674** (2000) 249.
- [20] W. Cassing, E. L. Bratkovskaya, and A. Sibirtsev, *Nucl. Phys. A* **691** (2001) 753.
- [21] J. Geiss *et al.*, *Phys. Lett. B* **447** (1999) 31.
- [22] W. Cassing and E. L. Bratkovskaya, *Nucl. Phys. A* **623** (1997) 570.
- [23] H. Weber, E. L. Bratkovskaya, W. Cassing, and H. Stöcker, *Phys. Rev. C* **67** (2003) 014904.
- [24] E. L. Bratkovskaya *et al.*, preprint nucl-th/0307098, *Phys. Rev. Lett.*, in press.
- [25] E. L. Bratkovskaya, M. Bleicher, W. Cassing, M. van Leeuwen, S. Soff, H. Stöcker, this volume.
- [26] H.-U. Bengtsson and T. Sjöstrand, *Comp. Phys. Commun.* **46** (1987) 43.
- [27] C. Spieles, R. Vogt, L. Gerland *et al.*, *J. Phys. G* **25** (1999) 2351.
- [28] E. L. Bratkovskaya, W. Cassing and H. Stöcker, *Phys. Rev. C* **67** (2003) 054905.
- [29] F. O. Duraes, H. Kim, S. H. Lee, F. S. Navarra, and M. Nielsen, *Phys. Rev. C* **68** (2003) 035208.
- [30] W. Cassing, L. A Kondratyuk, G. I. Lykasov, and M. V. Rzjanin, *Phys. Lett. B* **540** (2001) 1.
- [31] H. Satz, *Rep. Progr. Phys.* **63** (2000) 1511.
- [32] L. Grandchamp and R. Rapp, *Phys. Lett. B* **523** (2001) 60; *Nucl. Phys. A* **709** (2002) 415.
- [33] L. Ramello *et al.*, NA50 Collaboration, *Nucl. Phys. A* **715** (2003) 243c.
- [34] J. L. Nagle, PHENIX Collaboration, *Nucl. Phys. A* **715** (2003) 252.
- [35] W. Cassing, K. Gallmeister and C. Greiner, preprint hep-ph/0311358.
- [36] T. Falter *et al.*, preprint nucl-th/0303011; preprint nucl-th/0309057.
- [37] A. Airapetian *et al.*, *Eur. Phys. J. C* **21** (2001) 599; preprint hep-ex/0307023.
- [38] W. Cassing, E. L. Bratkovskaya, and O. Hansen, *Nucl. Phys. A* **707** (2002) 224.
- [39] J. W. Cronin *et al.*, *Phys. Rev. D* **11** (1975) 3105.
- [40] D. Antreasyan *et al.*, *Phys. Rev. D* **19** (1979) 764.
- [41] E. L. Bratkovskaya *et al.*, to be published.